

# Incremental stress-strain relation from granular elasticity: Comparison to experiments

Yimin Jiang<sup>1,2</sup> and Mario Liu<sup>1</sup><sup>1</sup>*Theoretische Physik, Universität Tübingen, 72076 Tübingen, Germany*<sup>2</sup>*Central South University, Changsha 410083, China*

(Received 11 June 2007; revised manuscript received 4 February 2008; published 28 February 2008)

Granular media are reversible and elastic if the stress increments are small enough. An elastic stress-strain relation, employed previously to determine static stress distributions, in this paper is compared to experiments by Kuwano and Jardine [Geotechnique **52**, 727 (2002)] on incremental stress-strain relations, and shown to yield satisfactory agreement. In addition, the yield condition is given a firmer footing.

DOI: [10.1103/PhysRevE.77.021306](https://doi.org/10.1103/PhysRevE.77.021306)

PACS number(s): 45.70.Mg, 81.40.Lm, 83.60.La, 46.05.+b

## I. INTRODUCTION

Grains slide and roll in granular media, in addition to being compressed and sheared. The strain associated with the former is frequently orders of magnitude larger, but only the latter, the elastic strain associated with deforming the grains, stores energy reversibly and maintains a static stress. Sliding and rolling are irreversible, plastic processes that only heat up the system. (Rolling is not itself irreversible, but the rotational energy is quickly lost when a grain crushes into its neighbors.) This observation indicates that it is the elastic strain  $u_{ij}$ , and not the total strain  $\varepsilon_{ij}$ , that is the relevant variable in granular media. We therefore take the granular energy as a function of the elastic strain,  $w = w(u_{ij})$ , the stress as its derivative,  $\sigma_{ij} = -\partial w / \partial u_{ij}$ , and refer to this approach as granular elasticity (GE). Given an explicit expression for  $w$ , one may then use  $\sigma_{ij} = \sigma_{ij}(u_{kl})$  to close the force balance, and calculate the static granular stress distributions of any desired geometry. Note the remarkable conclusion: The plastic part of the strain, though numerically dominant, is irrelevant for static stress fields.

When searching for an appropriate energy expression, it is important to keep the following fact in mind: Diverging compliance at diminishing compression is a basic characteristics of granular media, because it reflects the *geometric* fact that less material is being deformed. This is trivially true for the Hertzian contact between two grains, but also holds on larger scales. Therefore, the approximation of infinitely rigid grains is not a useful or realistic one for stress determination. A simple expression that will be given in Eq. (7) of the next section has this fact built in, and was previously shown to lead to realistic stress distributions in silos, sand piles, and sand banks subject to a point load [2].

These being indirect pieces of evidence, the question remains whether the elastic strain field  $u_{ij}$  may be directly measured. The answer is yes, and the method is equally suitable for experiment and simulation. The relevant observation is that plastic contributions do not always dominate the granular strain field. When probing the response of the total strain  $\delta\varepsilon_{ij}$  to a stress increment  $\delta\sigma_{kl}$ , the plastic portion decreases as the amplitude of the increments does, such that  $\delta\sigma_{ij} = M_{ijkl}\delta\varepsilon_{kl}$  holds with  $\delta\varepsilon_{kl} \approx \delta u_{kl}$ , and the elastic strain increment  $\delta u_{kl}$  becomes directly observable. This is plausible, as slips should be rare in the limit of vanishing increments. And this is borne out by experiments and simulations alike:

Kuwano and Jardine observed [1] that if the strain increments are kept below  $10^{-4}$ , the stress increments become reversible and incrementally linear (i.e., symmetric with respect to loading and unloading). In molecular-dynamics simulations, Alonso-Marroquin and Herrmann found the same behavior [3]: For strain changes around  $10^{-6}$ , the plastic contributions are around  $10^{-14}$ , smaller by eight orders of magnitude. This circumstance is very useful, because, given the energy  $w$ , we can calculate  $\delta\sigma_{ij} = (\partial\sigma_{ij} / \partial u_{kl})\delta u_{kl}$  and compare  $\partial\sigma_{ij} / \partial u_{kl} = \partial^2 w / \partial u_{ij} \partial u_{kl}$  with the measured  $M_{ijkl}$ . As we shall see, many measured features are reproduced, frequently with quantitative agreement. This is the main result of the present paper, and is rendered in Secs. IV and V. The yield behavior, as a result of an instability in the energy  $w$ , is discussed in Sec. III and the Appendix. The elastic part of the flow rule is considered in Sec. VI.

## II. GRANULAR ELASTICITY

The theory of isotropic linear elasticity is simple, consistent, and complete. It starts with an energy  $w$  that depends on the strain,  $u_{ij} = \frac{1}{2}(\nabla_i U_j + \nabla_j U_i)$ , with  $U_i$  the displacement vector,

$$w = K\Delta^2/2 + \mu u_s^2 \quad (\Delta \equiv -u_{\ell\ell}, \quad u_s \equiv \sqrt{u_{ij}^0 u_{ij}^0}); \quad (1)$$

see [4].  $K, \mu > 0$  are two material-dependent constants, referred to as the bulk and shear moduli. ( $u_{\ell\ell}$  is the trace of  $u_{ij}$ , and  $u_{ij}^0 \equiv u_{ij} - \frac{1}{3}u_{\ell\ell}\delta_{ij}$  its traceless part.) The stress-strain relation is obtained as a derivative,

$$\sigma_{ij} = -\partial w / \partial u_{ij} = K\Delta\delta_{ij} - 2\mu u_{ij}^0, \quad (2)$$

$$P \equiv \sigma_{\ell\ell}/3 = K\Delta, \quad \sigma_s \equiv \sqrt{\sigma_{ij}^0 \sigma_{ij}^0} = 2\mu u_s, \quad (3)$$

with the pressure  $P$  and shear stress  $\sigma_s$  being two frequently employed quantities. Some ramifications of isotropic linear elasticity are the following. (1) Since the stress  $\sigma_{ij}$  is given as a function of three variables  $U_i$ , the three components of the force balance  $\nabla_j \sigma_{ij} = \rho G_i$  (with  $\rho$  the density and  $G_i$  the gravitational constant) suffice to uniquely determine  $U_i$ , from which the stress  $\sigma_{ij}$  may be calculated for arbitrary geometry. (2) The inverse compliance tensor  $M_{ijkl}$  linking the increments of stress and strain,  $\delta\sigma_{ij}$  and  $\delta u_{kl}$ , is both isotropic and constant,

$$\delta\sigma_{ij} = \frac{\partial\sigma_{ij}}{\partial u_{k\ell}} \delta u_{k\ell} \equiv M_{ijk\ell} \delta u_{k\ell}, \quad (4)$$

$$M_{ijk\ell} = K \delta_{ij} \delta_{k\ell} - \mu (\delta_{ik} \delta_{j\ell} + \delta_{jk} \delta_{i\ell}). \quad (5)$$

(3) As the pressure  $P=K\Delta$  does not depend on the shear  $u_s$ , there is no volume dilatancy,  $(\partial P/\partial u_s)|_{\Delta}=0$ . (4) Yield is not predicted. [Note that while the points 2, 3, and 4 depend on the form of the energy  $w$ , the statement under (1) is quite general.]

These equations account well for isotropic elastic media, such as amorphous solids, but not for granular systems. Sand displays volume dilatancy, possesses a compliance tensor with significant stress-induced anisotropy, and, most importantly, never strays far from yield, displaying significant irreversible, fluidlike, plastic movements in its vicinity [5,6].

The first attempt to modify linear elasticity, so as to better account for granular behavior, was due to Boussinesq [7]. He assumed, around 1874, stress-dependent elastic moduli  $K, \mu \sim \Delta^{1/2} \sim P^{1/3}$  in Eq. (2),

$$\sigma_{ij} \sim \sqrt{\Delta} \left( \Delta \delta_{ij} - \frac{3-6\nu}{1+\nu} u_{ij}^0 \right), \quad \frac{3-6\nu}{1+\nu} = \frac{2\mu}{K}, \quad (6)$$

with  $\nu$  the constant Poisson ratio. This nonlinear stress-strain relation, sometimes referred to as the “quasielastic model,” is employed to understand granular compression [8] and sound velocity [9]. Unfortunately, the above fault list of linear elasticity remains partly intact: (a) As  $P$  remains a function of  $\Delta$  alone, dilatancy vanishes,  $\partial P/\partial u_s|_{\Delta}=0$ , and (b) yield must still be postulated. Worst of all, no energy  $w$  exists such that  $\sigma_{ij} = -\partial w/\partial u_{ij}$  holds (this may be demonstrated by showing that the associated Maxwell relation is violated,  $\partial\sigma_{ij}/\partial u_{k\ell} \neq \partial\sigma_{k\ell}/\partial u_{ij}$ ).

Therefore, we choose to start from the energy [10]

$$w = \sqrt{\Delta} (\mathcal{B} \frac{2}{5} \Delta^2 + \mathcal{A} u_s^2) = \mathcal{B} \sqrt{\Delta} (\frac{2}{5} \Delta^2 + u_s^2/\xi), \quad (7)$$

with  $\mathcal{A}, \mathcal{B} > 0$  denoting two density-dependent material constants, and  $\xi \equiv \mathcal{B}/\mathcal{A}$ . The associated stress is

$$\sigma_{ij} = \sqrt{\Delta} (\mathcal{B} \Delta \delta_{ij} - 2\mathcal{A} u_{ij}^0) + \mathcal{A} \frac{u_s^2}{2\sqrt{\Delta}} \delta_{ij}. \quad (8)$$

These two expressions define what we refer to as granular elasticity. When compared to Eq. (6), the only difference is the last term  $\sim u_s^2/\sqrt{\Delta}$ , which, however, is amazingly useful in accounting for granular behavior. It yields volume dilatancy and shear-induced anisotropy, and, above all, predicts yield at the Coulomb condition

$$\sigma_s/P = \sqrt{2\mathcal{A}/\mathcal{B}} = \sqrt{2/\xi}. \quad (9)$$

Moreover, solving the force balance equation  $\nabla_j \sigma_{ij} = \nabla_j \pi_{ij} = \rho G_i$  for three classical cases, silos, sand piles, and a granular bank under a point load, we find Eq. (8) to result in rather satisfactory agreement with experiments (see [2]).

In Ref. [1], Kuwano and Jardine measured  $\delta\sigma_{ij}$  and  $\delta u_{k\ell}$  independently, obtaining the matrix  $M_{ijk\ell}$  connecting them,  $\delta\sigma_{ij} = M_{ijk\ell} \delta u_{k\ell}$ . The data in Ref. [1] are extensive, comprising 36 components of  $M_{ijk\ell}$ , all as functions of pressure, shear, and the void ratio  $e$ . (There are empirical rules for

these components in soil mechanics, which the authors found to be well satisfied. When these are employed, only five independent coefficients are left.) In this paper, we compare these data—including the empirical rules—to  $\partial\sigma_{ij}/\partial u_{k\ell}$  as calculated from Eq. (8). It represents an ambitious test of the energy  $w$ , Eq. (7): The energy and stress of Eqs. (7) and (8) depend only on two material parameters  $\mathcal{A}$  and  $\mathcal{B}$ , with their ratio fixed by the yield condition, Eq. (9). Since the Ham River sand used in the experiment has a Coulomb yield angle of around  $28^\circ$ , implying  $\xi \equiv \mathcal{B}/\mathcal{A} = 5/3$ , only  $\mathcal{A}$ , a scale factor and a measure of the total stiffness, is left as an adjustable parameter. Taking  $\mathcal{A} = 5100$  MPa, we find satisfactory agreement with the data of [1] at all values of pressure and shear, for the void ratio  $e = 0.66$ —except close to yield, which, due to increased plastic contributions, represents an especially difficult experimental regime. Because Kuwano and Jardine noticed that  $e$  alters only the total stiffness, by the factor  $f \equiv (2.17 - e)^2/(1 + e)$ , taking  $\mathcal{A}, \mathcal{B} \sim f$  achieves agreement with respect to any other values of  $e$  as well. Similar agreement to their data on ballotini (glass beads) was achieved by taking  $\mathcal{A} = 4200$  MPa. To summarize, we take

$$\mathcal{A} = \mathcal{A}_0 \times \frac{(2.17 - e)^2}{1.3736(1 + e)}, \quad \xi \equiv \frac{\mathcal{B}}{\mathcal{A}} = \frac{5}{3}, \quad (10)$$

with  $\mathcal{A}_0 = 5100$  and  $4200$  MPa being the values of  $\mathcal{A}$  for  $e = 0.66$ , for Ham River sand and ballotini, respectively.

Finally, some remarks. First we consider the subtle question of whether a reference state exists given the predominantly plastic nature of the displacement. For the following reasons we believe it does. Forgetting for a moment the gravitation, and dividing the total displacement into two parts  $\vec{U}^{\text{tot}} = \vec{U} + \vec{U}^p$ , because the elastic displacement  $\vec{U}$  is the portion that changes the energy reversibly, any state that does not possess elastic energy and is not subject to any external stresses—implying a vanishing  $\vec{U}$ —is a valid reference state. (That such a reference state may not be stable does not appear to constitute a legitimate worry, because it can always be stabilized by an arbitrarily small but finite external pressure.) There are innumerable reference states, all connected by purely plastic displacements. If a reference state is deformed by slowly increasing the stress, the total displacement will contain both elastic and plastic contributions. If we change the reference state by the same plastic displacement, the new reference state is separated from the deformed state by a purely elastic displacement. Since such an *evolving reference state* exists for every stressed state, elastic displacements remain well defined in spite of arbitrarily strong plastic motions. (Turning on the gravitation simply renders the internal stress nonuniform. The same conclusion holds.)

Second, we consider *inherent*, or *fabric*, *anisotropy*, a well-known phenomenon in soil mechanics: Sand is sometimes anisotropic even when subject to isotropic stresses. We believe that this is primarily due to density inhomogeneities: Since the elastic coefficients  $\mathcal{A}, \mathcal{B}$  are density dependent, a nonuniform density indeed renders the system’s response anisotropic whatever the stress is. Note that the density gets jammed at formation, and any inhomogeneities will remain forever if unperturbed. In fact, the central dip in the bottom

pressure of sand piles may well be understood by assuming that some procedures applied to form the piles produce non-uniform density fields (see [2]). Similar inhomogeneities may also result from avalanches. This is the reason we decided, as a first step, to neglect any other conceivable reasons for fabric anisotropy, taking strain and density as the only variables of GE. Should agreement between theoretical predictions and experimental data prove elusive in some cases, necessitating the inclusion of more variables, our strategy should nevertheless give us better ideas of what this variable is, where its main influence lies, and how large it is.

### III. YIELD AND ENERGETIC INSTABILITY

Any macroscopic energy must be a convex function of its state variables to ensure stability—this is why compressibility and specific heat are always positive (cf. [11]). Being a quadratic function of  $\Delta$  and  $u_s$ , the energy of linear elasticity, Eq. (1), is always convex. Conversely, the granular energy, Eq. (7), is convex if and only if

$$(\partial^2 w / \partial \Delta^2)_{u_s} \geq 0, \quad (\partial^2 w / \partial u_s^2)_{\Delta} \geq 0, \quad (11)$$

$$(\partial^2 w / \partial \Delta \partial u_s)^2 \leq (\partial^2 w / \partial \Delta^2)_{u_s} (\partial^2 w / \partial u_s^2)_{\Delta} \quad (12)$$

hold. (See the Appendix for some subtleties in this context.) More explicitly, this implies

$$u_s^2 / \Delta^2 \leq 2B/A, \quad (13)$$

drawing the boundary for the region of stable strains. Deriving  $4P/\sigma_s = (\Delta/u_s) \times (2B/A + u_s^2/\Delta^2)$  from Eq. (8), and inserting  $u_s^2/\Delta^2 = 2B/A$  into it, Eq. (9), the Drucker-Prager version of the Coulomb yield condition (cf. [13,14]) is obtained. The actual Coulomb yield condition  $\sigma_s/P = (\sqrt{18+6L^2 \sin \varphi_c}) / (L \sin \varphi_c + 3)$ , where  $L \equiv \sqrt{3} \tan[\frac{1}{3} \arcsin(\sqrt{6} \sigma_{ij}^0 \sigma_{jk}^0 \sigma_{ki}^0 / \sigma_s^3)]$  denotes the Lode parameter, will result only if terms  $\sim u_{ij}^0 u_{jk}^0 u_{ki}^0$  are included in Eq. (7).

In a classic paper, Goddard [9] started from Hertz contacts between grains, and considered the structure of the energy and stress. He concluded that, if the topology of the grain contacts does not change with stress, the energy is a homogeneous function of degree 5/2 in the strain  $u_{ij}$ , of the form  $w = \Delta^{2.5} g(u_s^2/\Delta^2, u_{ij}^0 u_{jk}^0 u_{ki}^0 / \Delta^3)$ , where  $g$  is an arbitrary function. As Eq. (7) is clearly a special case of this general energy, we take this as a further, microscopically founded, support for our starting point.

There is an instructive analogy between the granular stress-strain relation, Eq. (8), and the van der Waals equation of state for real gases. Boyle's law is stable everywhere while the van der Waals equation has a nonphysical zone, the liquid-gas instability, in which the compressibility is negative. Similarly, Hooke's law is stable everywhere, but the granular stress-strain relation has a forbidden region, that of yield. Note that

$$\partial P / \partial \Delta |_{\sigma_s} \geq 0 \quad (14)$$

is implied by Eqs. (11) and (12) (see the Appendix), so this forbidden region is also characterized by a negative com-

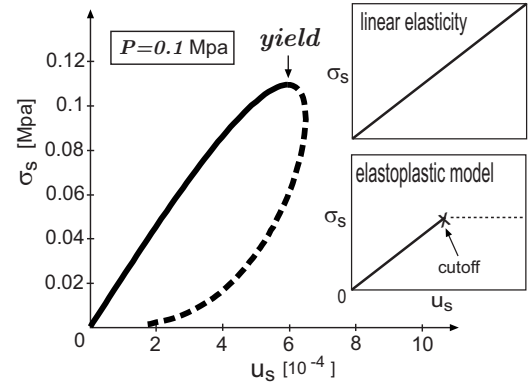


FIG. 1. Shear stress vs shear strain for given pressure: for GE, linear elasticity, and elastoplastic theory (upper and lower insets).

pressibility. The actual innovation of the van der Waals theory is the fact that the condition for the onset of the liquid-gas transition, instead of being an extra input, is implied by the free energy. Similarly, yield is now implied by Eq. (7).

### IV. GRANULAR STRESS-STRAIN RELATION

The granular stress-strain relation Eq. (8) and the definitions of Eq. (3) imply

$$P = \Delta^{3/2} (\mathcal{B} + \frac{1}{2} \mathcal{A} u_s^2 / \Delta^2), \quad (15)$$

$$\sigma_s = 2\mathcal{A} \Delta^{1/2} u_s. \quad (16)$$

Eliminating  $\Delta$ , we obtain

$$\mathcal{B} \sigma_s^4 - 8\mathcal{A}^3 P u_s^3 \sigma_s + 8\mathcal{A}^5 u_s^6 = 0. \quad (17)$$

Figure 1 plots  $\sigma_s$  vs  $u_s$  for the fixed pressure of  $P = 0.1$  MPa. Note how remarkably linear the plot is—almost until yield, where the curve turns back abruptly. (Dashed lines are used throughout for unstable states.) This behavior is approximated by the elastoplastic model, frequently used in soil mechanics: linear elasticity followed by yield and flat plastic motion; see the lower insets in Fig. 1. Nonlinearity in shear is relevant only when yield is close.

If instead  $u_s$  is eliminated from Eqs. (15) and (16), the expression

$$\sigma_s^2 + 8\mathcal{A} \mathcal{B} \Delta^3 - 8\mathcal{A} P \Delta^{3/2} = 0 \quad (18)$$

allows a plot of pressure  $P$  vs compression  $\Delta$ , at given  $\sigma_s = 0.1$  MPa; see Fig. 2. The pressure increases with the compression, implying a positive compressibility, only in the region of large  $\Delta$ . The compressibility is negative where  $\Delta$  is small, and the stability condition, Eq. (9) or (14), is violated. The van der Waals equation of state,  $(P - a/v^2)(v - b) = RT$ , is quite similar, where  $1/v$  corresponds to  $\Delta$ ,  $R$  is the gas constant, and  $v$  the molar volume; see, e.g., [11]. The system can be in either the dense liquid state or the rarefied gaseous phase, with the zone in between forbidden; see inset of Fig. 2.

Alternatively, we may plot  $\Delta$  vs  $u_s$  at fixed  $P$ , or  $P$  vs  $\sigma_s$  at fixed  $\Delta$ ; see Figs. 3 and 4, both showing clear evidence of

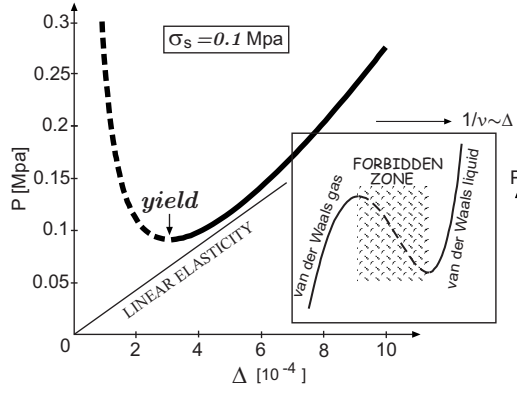


FIG. 2. Thick line: Pressure vs compression at fixed shear for GE. (Dashed lines represent unstable states.) Thin straight line: The same curve for linear elasticity. Inset: The analogous instability in the isothermal curve of the van der Waals equation of state.

“volume dilatancy,” the fact (first noticed by Reynolds) that granular systems expand with shear, or  $\partial\Delta/\partial u_s|_P \neq 0$  or  $\partial P/\partial\sigma_s|_\Delta \neq 0$ . For linear elasticity, these plots are simply horizontal, and the derivatives vanish. If the Boussinesq model Eq. (6) were employed, all four plots would be much harder to distinguish from those of linear elasticity. So the last term of Eq. (8) is indeed essential. (Plastic motion, not considered here, contributes to additional dilatancy, and may dominate.)

Hooke’s law Eq. (2),  $\sigma_{ij} = K\Delta\delta_{ij} - 2\mu u_{ij}^0$ , may be written as

$$u_{ij} = \frac{\nu}{E}\sigma_{mn}\delta_{ij} - \frac{\sigma_{ij}}{2\mu}, \quad (19)$$

with the Poisson ratio  $\nu$  and the Young modulus  $E$  given as

$$E = \frac{9\mu K}{3K + \mu}, \quad \nu = \frac{3K - 2\mu}{6K + 2\mu}. \quad (20)$$

If the granular stress-strain relation Eq. (8) is required to assume these familiar forms, either Eq. (2) or Eq. (19) leads to strain dependency of  $K, \mu$ ,

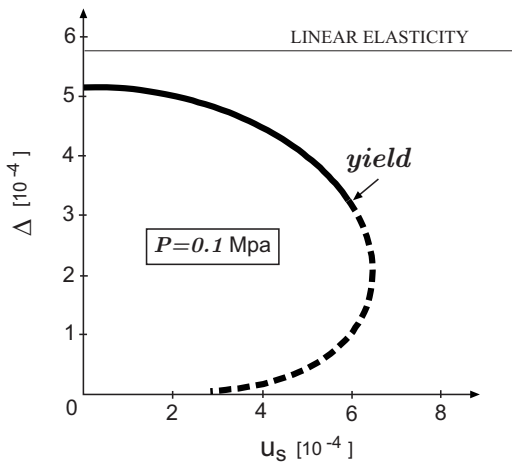


FIG. 3. Compression  $\Delta$  vs shear strain  $u_s$ , at fixed pressure, for GE. The dashed line is again unstable. In linear elasticity, the same curve is a horizontal straight line.

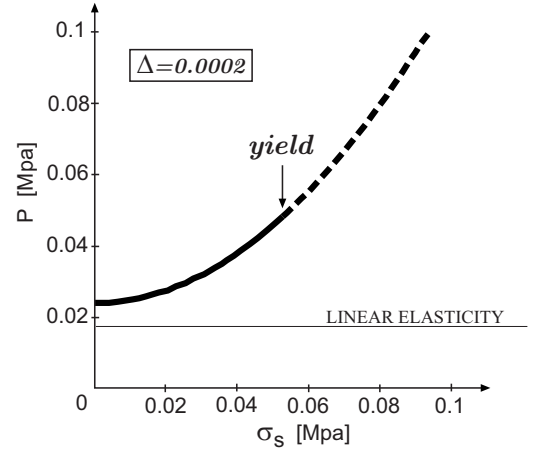


FIG. 4. Pressure  $P$  vs shear stress  $\sigma_s$ , at fixed compression, for GE. The dashed line is unstable. In linear elasticity, the same curve is a horizontal straight line.

$$K = \Delta^{1/2}(\mathcal{B} + \frac{1}{2}\mathcal{A}u_s^2/\Delta^2), \quad (21)$$

$$\mu = \mathcal{A}\Delta^{1/2}, \quad (22)$$

and via Eq. (20) also of  $E, \nu$ . As this is an intuitive way to characterize nonlinear elastic behavior, we shall consider their shear and pressure dependency more closely here. Using Eqs. (15) and (16), we write these moduli as

$$\mu = \tilde{\mu}\xi^{1/3}, \quad K = \tilde{K}\xi^{-2/3},$$

$$E = \tilde{E}\frac{3\mathcal{B} + \mathcal{A}}{3\mathcal{B} + \mathcal{A}\xi}\xi^{1/3}, \quad \nu = \frac{3\mathcal{B} - 2\mathcal{A}\xi}{6\mathcal{B} + 2\mathcal{A}\xi}, \quad (23)$$

where  $\xi$  quantifies shear,

$$\xi = \frac{1}{2}[1 \pm \sqrt{1 - (\mathcal{B}/2\mathcal{A})(\sigma_s/P)^2}], \quad (24)$$

and  $\tilde{\mu}, \tilde{K}, \tilde{E}$ , and  $\tilde{\nu}$  denote the corresponding values without shear, at  $\xi=1$ ,

$$\tilde{\mu} = \mathcal{A}\left(\frac{P}{\mathcal{B}}\right)^{1/3}, \quad \tilde{K} = \mathcal{B}\left(\frac{P}{\mathcal{B}}\right)^{1/3}, \quad \tilde{E} = \frac{9\mathcal{A}\mathcal{B}}{3\mathcal{B} + \mathcal{A}}\left(\frac{P}{\mathcal{B}}\right)^{1/3} \quad (25)$$

(see Fig. 5). [The positive sign in Eq. (24) is the stable branch, which meets the unstable branch with the negative sign at yield, where the square root vanishes.]

As mentioned in the Introduction, the  $P^{1/3}$  dependence of the characters with tildes is well known. For typical granular behavior, however, the more relevant dependence is that on shear, which derives—as for yield and dilatancy—from the last term of Eq. (8).

## V. THE COMPLIANCE TENSOR

### A. Theoretical expressions

Starting from Eq. (8), the tensor  $M_{ijkl}$  of Eq. (4) is calculated as

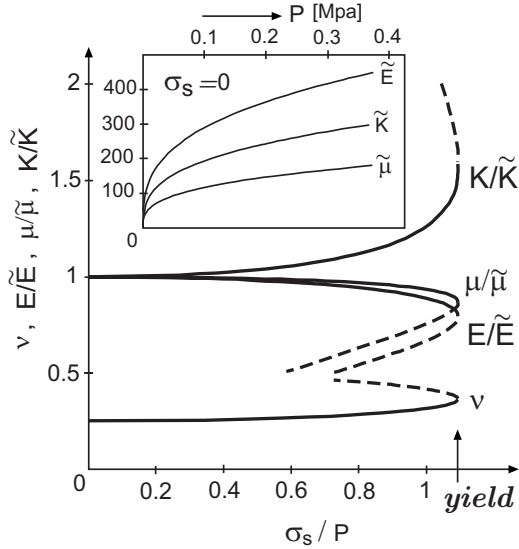


FIG. 5. Variations of  $K, \mu, E, \nu$  with  $\sigma_s/P$  for GE. The moduli are rescaled by their values at  $\sigma_s=0$ , denoted with a tilde. Their variation  $\sim P^{1/3}$  is shown in the inset.

$$M_{ijkl} = \mathcal{A} \sqrt{\Delta} [(u_s^2/4\Delta^2 + 4/3 - 3B/2A) \delta_{ij} \delta_{kl} - \delta_{ik} \delta_{jl} - \delta_{il} \delta_{jk} + (u_{ij} \delta_{kl} + \delta_{ij} u_{kl})/\Delta]. \quad (26)$$

The compliance tensor  $\lambda_{ijkl}$ , defined via

$$du_{ij} = \lambda_{ijkl} d\sigma_{kl}, \quad (27)$$

is obtained by inverting  $M_{ijkl}$ ,

$$\begin{aligned} \lambda_{ijkl} &= \frac{[\mathcal{A}u_s^2 + 2(\mathcal{A} - B)\Delta^2] \delta_{kl} \delta_{ij}}{6\mathcal{A}\Delta^{1/2}(\mathcal{A}u_s^2 - 2B\Delta^2)} - \frac{\delta_{ik} \delta_{jl} + \delta_{il} \delta_{jk}}{4\mathcal{A}\Delta^{1/2}} \\ &+ \frac{u_{ij}\Delta \delta_{kl} + u_{kl}\Delta \delta_{ij} + u_{ij}u_{kl}}{3\Delta^{1/2}(\mathcal{A}u_s^2 - 2B\Delta^2)} \\ &= \frac{9\mathcal{A}^5\sigma_s^2 + 8(4\mathcal{A} - 9B)\mu^6}{54\mu(\mathcal{A}^5\sigma_s^2 - 8\mu^6B)} \delta_{kl} \delta_{ij} - \frac{\delta_{ik} \delta_{jl} + \delta_{il} \delta_{jk}}{4\mu} \\ &- \frac{4\mathcal{A}^3\mu^3(\sigma_{ij}^0 \delta_{kl} + \sigma_{kl}^0 \delta_{ij}) - 3\mathcal{A}^5\sigma_{ij}^0 \sigma_{kl}^0}{9\mu(\mathcal{A}^5\sigma_s^2 - 8\mu^6B)}. \end{aligned} \quad (28) \quad (29)$$

In Eq. (28)  $\lambda_{ijkl}$  is strain and in Eq. (29) stress dependent—where the conversion is calculated using  $\Delta = \mu^2/\mathcal{A}^2$ ,  $u_{ij}^0 = -\frac{1}{2}\sigma_{ij}^0/\mu$ ,  $u_s = \frac{1}{2}\sigma_s/\mu$ , with  $\mu = \mathcal{A}(\xi P/B)^{1/3}$  [cf. Eqs. (23) and (25)]. Equation (29)—surprisingly complicated if the starting expression for the energy serves as a benchmark—is what may be compared to experiments directly.

Before we do this, it is useful to pause and notice that the last term of both Eqs. (26) and (29) deviates structurally from the isotropic form of Eq. (5). More generally, for an isotropic medium and in the presence of pure compression ( $\sigma_{ij}^0=0$ ,  $P \neq 0$ ), we may (quite independently of the specific form of the elastic energy) take  $\lambda_{ijkl}$  to be

$$\lambda_{ijkl}^0 = \lambda_1 \delta_{ij} \delta_{kl} + \lambda_2 (\delta_{ik} \delta_{jl} + \delta_{il} \delta_{jk}), \quad (30)$$

with  $\lambda_1, \lambda_2$  arbitrary scalar functions of  $\Delta, u_s$ , and the Lode parameter  $L$ . This is because both  $\sigma_{ij}$  and  $u_{kl}$  are symmetric, and hence  $\lambda_{ijkl} = \lambda_{jikl} = \lambda_{ijlk}$ ; and the Maxwell relation holds,  $\partial^2 w / \partial u_{ij} \partial u_{lk} = \partial^2 w / \partial u_{lk} \partial u_{ij}$ , so that  $\lambda_{ijkl} = \lambda_{klij}$ . In the presence of shear,  $\sigma_{ij}^0 \neq 0$ ,  $\lambda_{ijkl}$  can take on many more terms. To linear order in  $\sigma_{ij}^0$ , these are

$$\lambda_3 (\sigma_{ij}^0 \delta_{kl} + \delta_{ij} \sigma_{kl}^0) + \lambda_4 (\sigma_{ik}^0 \delta_{jl} + \sigma_{il}^0 \delta_{jk} + \sigma_{jl}^0 \delta_{ik} + \sigma_{jk}^0 \delta_{il}).$$

To second order, we may substitute all the above  $\sigma_{ij}^0$  with  $\sigma_{ik}^0 \sigma_{kj}^0$ , and also add the terms  $\sigma_{ij}^0 \sigma_{kl}^0$  and  $\sigma_{ik}^0 \sigma_{jl}^0 + \sigma_{jk}^0 \sigma_{il}^0$ . We shall refer to  $\lambda_{ijkl}^0$  as being isotropic, and the  $\sigma_{ij}^0$ -dependent ones as displaying “shear-induced anisotropy.” If the medium is inherently anisotropic, say because the grains are pressed into some quasiperiodic array, leading to a preferred direction  $\vec{n}$ , the above expression is more complicated, because  $\delta_{ij}$  in Eq. (30) may now be substituted by three different tensors:  $\delta_{ij} - n_i n_j$ ,  $n_i n_j$ , and  $\varepsilon_{ijk} n_k$ . For triclinic symmetry and without the Maxwell relation, all 36 elements of  $\lambda_{ijkl}$  are independent—even in the absence of shear. As mentioned, this fabric anisotropy is not included in the present consideration, because the starting expression for the energy, Eq. (7), is isotropic.

## B. Comparison with experiments

Because  $\sigma_{ij}$  and  $u_{ij}$  are symmetric, each characterized by six independent components, Eq. (27) may be written as a vector equation  $d\vec{u} = \hat{\lambda} d\vec{\sigma}$ , with  $\hat{\lambda}$  a  $6 \times 6$  matrix, and  $du, d\sigma$  given as in Eq. (31). In the so-called “principal system” of coordinates, in which  $\sigma_{ij}$  is diagonal (but not  $d\sigma_{ij}$ ), Kuwano and Jardine take this vector equation to be given as [1]

$$\begin{pmatrix} du_{11} \\ du_{22} \\ du_{33} \\ 2du_{23} \\ 2du_{13} \\ 2du_{12} \end{pmatrix} = \begin{pmatrix} 0 & 0 & 0 \\ \hat{C} & 0 & 0 \\ 0 & 0 & 0 \\ 0 & 0 & 0 \\ 0 & 0 & 0 \\ 0 & 0 & 0 \end{pmatrix} \begin{pmatrix} d\sigma_{11} \\ d\sigma_{22} \\ d\sigma_{33} \\ -d\sigma_{23} \\ -d\sigma_{13} \\ -d\sigma_{12} \end{pmatrix} \quad (31)$$

with

$$\hat{C} = \begin{pmatrix} -1/E_1 & \nu_{12}/E_2 & \nu_{13}/E_3 \\ \nu_{21}/E_1 & -1/E_2 & \nu_{23}/E_3 \\ \nu_{31}/E_1 & \nu_{32}/E_2 & -1/E_3 \end{pmatrix}. \quad (32)$$

$G_{ij}$  is referred to as the shear modulus in the  $i$ - $j$  plane,  $E_i$  the Young modulus along  $i$ , and  $\nu_{ij}$  the Poisson ratio for the effect of the  $i$  strain on the  $j$  strain. Identifying these moduli with components of the  $\lambda_{ijkl}$  tensor,

$$G_{ij} = -1/4\lambda_{ijij},$$

$$E_i = -1/\lambda_{iiii},$$

$$\nu_{ij} = -\lambda_{ijj}/\lambda_{jjj} \quad (33)$$

(for  $i \neq j$  and without summation over  $i$  or  $j$ ), we may employ Eq. (29) to obtain

$$G_{13} = G_{23} = G_{12} = \mu, \quad (34)$$

$$E_i = \frac{27\mu(A^5\sigma_s^2 - 8\mu^6B)}{9A^5\sigma_s^2 - 72\mu^6B - As_i^2}, \quad (35)$$

$$\nu_{ij} = \frac{1}{2} \frac{9A^5\sigma_s^2 - 72\mu^6B + 2As_i s_j}{9A^5\sigma_s^2 - 72\mu^6B - As_j^2}, \quad (36)$$

with  $\mu = \mathcal{A}(\xi P/B)^{1/3}$ ,  $s_i \equiv 3A^2\sigma_i^0 - 4\mu^3$ ,  $\sigma_i^0 \equiv \sigma_i - P$ , and  $\sigma_i$  denoting the three diagonal components of  $\sigma_{ij}$  in the principal system. Before embarking on a comparison, we shall first establish a few qualitative features from theory. (1) Without shear,  $\sigma_i^0 \rightarrow 0$ , all  $E_i$  are equal,

$$E_i \rightarrow E_{\text{sec}} = \frac{27AB}{2A + 9B} \left(\frac{P}{B}\right)^{1/3}, \quad (37)$$

where  $E_{\text{sec}}$  is called the secant Young modulus. The same holds for the Poisson ratios,

$$\nu_{ij} \rightarrow \tilde{\nu}^* = \frac{1}{2} \frac{9B - 4A}{9B + 2A}. \quad (38)$$

[Note that  $\tilde{\nu}^* = (22/17)\tilde{\nu}$  and  $E_{\text{sec}} = (18/17)\tilde{E}$ .] (2) Because of Eq. (30) and irrespective of the energy specified (for an isotropic medium), we have  $E_1 = E_2 = E_3$ ,  $\nu_{12} = \nu_{13} = \nu_{23}$ , and  $G_{12} = G_{13} = G_{23}$  in the absence of shear,  $\sigma_{ij}^0 = 0$ . Any discrepancy with experiment therefore may imply fabric anisotropy. (3) Finite shear will split  $E_i$  and  $\nu_{ij}$ , but not  $G_{ij}$ ; cf. Eq. (34)—though this is an energy-related feature. (4) Because of the Maxwell relation, the matrix  $\hat{\lambda}$  of Eq. (31) is symmetric, implying especially (no summation)

$$\nu_{ij}E_i = \nu_{ji}E_j. \quad (39)$$

This symmetry was noted by Love [15] and adopted by Kuwano and Jardine in interpreting their data [1]. (5) The moduli  $E$ ,  $\mu$ , and  $\nu$  are related as  $E = 2\mu(\nu + 1)$ ; see Eqs. (20). A similar relation holds for  $\mu$ ,  $E_i$ , and  $\nu_{ik}$  [no summation, see Eqs. (35) and (36)],

$$E_i(6\mu\nu_{ij} - E_j)^2 = 4E_j(3\mu - E_i)(3\mu - E_j). \quad (40)$$

It is important to realize that all formulas of this section hold not only for Cartesian coordinates,  $i \rightarrow x, y, z$ , but also for cylindrical ones,  $i \rightarrow z, \rho, \varphi$ . Taking  $\Delta = u_{\varphi\varphi} + u_{\rho\rho} + u_{zz}$ , and similarly for  $u_s$ , we may again start from the same energy, Eq. (7), and derive all the results here. (Spatial differentiation is what mars the similarity. Yet once the strain components  $u_{\rho\rho}, u_{\rho\varphi}, \dots$  are given, no spatial differentiation is needed.) The one difference is that, for any constant  $\sigma_{ij}$  in Cartesian coordinates, there is always a principal system. In cylindrical coordinates, this holds only if the stress is also cylindrically symmetric. In other words, only if the stress is uniaxially diagonal,  $\sigma_{ij} = \text{diag}(\sigma_1, \sigma_2, \sigma_3)$  with  $\sigma_2 = \sigma_1$  in Cartesian coordinates, will it be diagonal cylindrically.

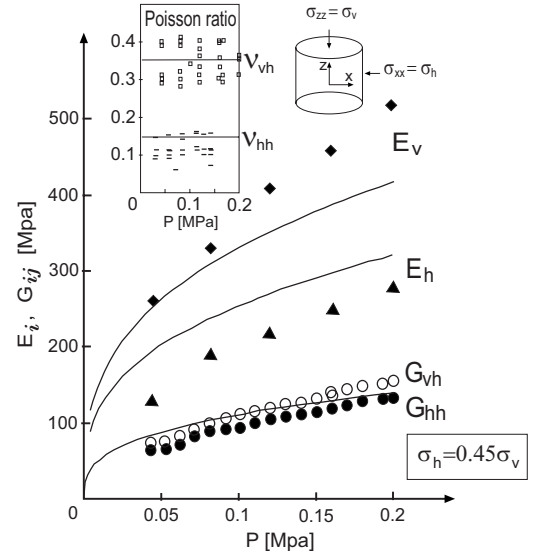


FIG. 6. Variation with pressure  $P$  of the shear moduli  $G_{vh}, G_{hh}$ , Young moduli  $E_v, E_h$ , and Poisson ratios  $\nu_{vh}, \nu_{hh}$  (inset), at  $\sigma_h/\sigma_v = 0.45$  for GE. Symbols (squares, triangles, spheres, and filled spheres) are the same data for Ham River sand from [1], at a void ratio of 0.66.

Because Kuwano and Jardine [1] used an axial-symmetric device for their measurements, the stress they apply is indeed cylindrically symmetric, with:  $G_{\rho z} = G_{\varphi z}$ ,  $E_\rho = E_\varphi$ ,  $\nu_{\rho z} = \nu_{\varphi z}$ , and  $\nu_{z\rho} = \nu_{z\varphi}$  [cf. Eqs. (34)–(36) noting that  $s_\rho = s_\varphi$ ]. In addition, Eq. (39) leads to  $\nu_{\rho\varphi} = \nu_{\varphi\rho}$ . Following [1], we refer to the response coefficients being measured as  $G_{hh} \equiv G_{\rho\rho}$ ,  $G_{vh} \equiv G_{\rho z} = G_{\varphi z}$ ,  $E_h \equiv E_\rho = E_\varphi$ ,  $E_v \equiv E_z$ ,  $\nu_{hh} \equiv \nu_{\rho\rho} = \nu_{\varphi\rho} = \nu_{\varphi\varphi}$ ,  $\nu_{hv} \equiv \nu_{\rho z} = \nu_{\varphi z}$ , and  $\nu_{vh} \equiv \nu_{z\rho} = \nu_{z\varphi}$ , where  $h$  is the horizontal direction, either  $\rho$  or  $\varphi$ , and  $v$  the vertical direction  $z$ ; see the cylinder of Fig. 6. (These are seven coefficients characterizing the independent five mentioned in the Introduction.) The main plots of Fig. 6 compare the theoretical curve [calculated by taking  $\sigma_\rho = \sigma_\varphi = \sigma_h$  and  $\sigma_z = \sigma_v$  in Eqs. (34)–(36)] and the experimental data (measured with Ham River sand) of  $E_h, E_v, G_{vh}$ , and  $G_{hh}$ , as functions of  $P$ , for  $\sigma_h = 0.45\sigma_v$ . The inset shows the same comparison for  $\nu_{vh}$  and  $\nu_{hh}$ . We especially note that theory and experiment agree on the ordering of the induced anisotropy, i.e.,  $\nu_{vh} > \nu_{hh}$ ,  $E_v > E_h$ , and  $G_{hh} \approx G_{vh}$ , which are pairwise equal in linear elasticity and the Bousinesq model. (The slight difference between  $G_{hh}$  and  $G_{vh}$  may be the result of weak fabric anisotropy.) All in all, for a theory without any useful fit parameter, the agreement must be considered at least a promising first step of the elastic approach.

Kuwano and Jardine [1] employ the following empirical formulas (in MPa) for the Ham River sand,

$$E_v = 204f(\sigma_v/P_a)^{0.52}, \quad (41)$$

$$E_h = 174f(\sigma_h/P_a)^{0.53}, \quad (42)$$

$$G_{vh} = 72f(\sigma_v/P_a)^{0.32}(\sigma_h/P_a)^{0.2}, \quad (43)$$

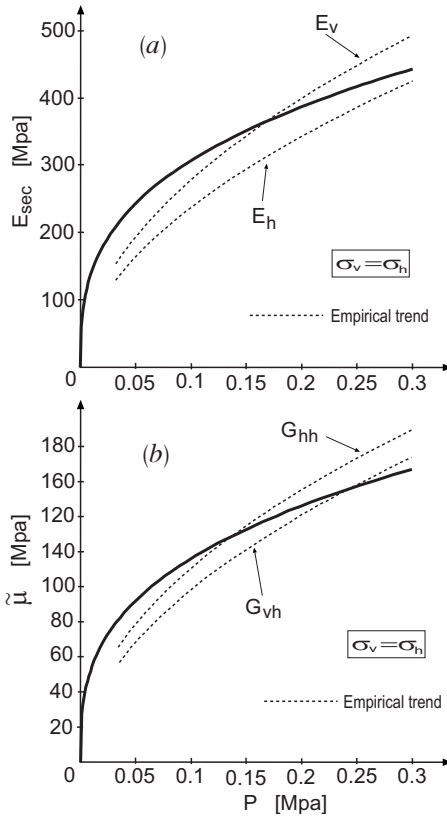


FIG. 7. Solid lines present the variation of the Young and shear moduli,  $E_{sec}$  and  $\mu$ , with the pressure  $P$ , for the case of vanishing shear,  $\sigma_v = \sigma_h$ , as calculated from GE. The dotted lines are the empirical formula of Kuwano and Jardine [1], for Ham River sand at the void ratio  $e=0.66$ . If density inhomogeneity can be ruled out, the split may be indicative of fabric anisotropy.

$$G_{hh} = 81f(\sigma_v/P_a)^{-0.04}(\sigma_h/P_a)^{0.53}, \quad (44)$$

where  $P_a=0.1013$  MPa is the atmospheric pressure and  $f = (2.17 - e)^2 / (1 + e)$ . ( $f=1.3736$  for the void ratio  $e=0.66$ .) Figure 7 shows the theoretical and experimental values for  $E_h$ ,  $E_v$ ,  $G_{vh}$ , and  $G_{hh}$ , as functions of  $P$ , for the isotropic case  $\sigma_h = \sigma_v$ . The fact that  $E_h, E_v$  and  $G_{vh}, G_{hh}$  are pairwise different may indicate some fabric anisotropy. Moreover, the theoretical curves are  $\sim P^{1/3}$ , yet the experimental ones seem to suggest a larger power:  $\sim P^{1/2}$ . As discussed, this is a known contradiction between Hertz contact and sound data, with possible explanations provided by Goddard [9] and de Gennes [12], and a question of simplicity vs accuracy in the present approach.

Figure 8 displays the effect of shear on different moduli, with  $\sigma_h \neq \sigma_v$ . The upper, middle, and lower figures, respectively, plot the Young moduli  $E_i$ , the shear modulus  $\mu$  (both scaled by their isotropic values  $E_{sec}$  and  $\tilde{\mu}$ ), and the Poisson ratios  $\nu_{ij}$ . In agreement with the empirical formulas Eqs. (41)–(44),  $E_v$  increases with  $\sigma_s/P$ , while  $E_h$  decreases, in the region away from yield. As yield is approached, both drop quickly to zero. This critical preyield behavior is clearly absent for the empirical formulas and is of interest for future experiments. In theory,  $G_{vh}$  and  $G_{hh}$  are equal, decreasing with  $\sigma_s/P$  moderately, by less than 20%. In experiments, the

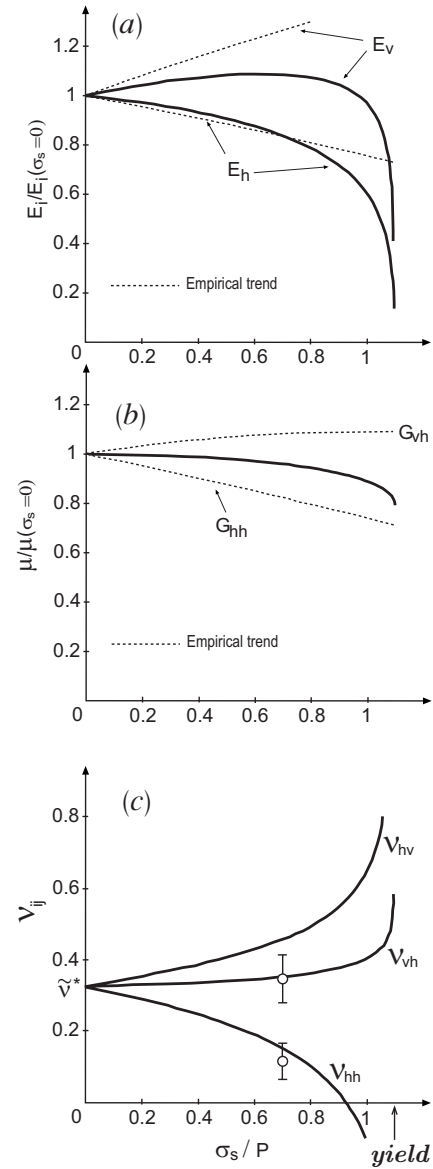


FIG. 8. Solid lines of the upper, middle, and lower figures show the Young moduli, shear moduli, and Poisson ratios, respectively, calculated from GE as functions of  $\sigma_s/P$ . The dotted lines present the empirical formulas of [1] for the Ham River sand, at  $e=0.66$ .

shear moduli are split, with one increasing, the other decreasing. The discrepancy between the theory and experiment is in the range from  $\sigma_s/P=0$  to 0.6 within 20%.

Variation of the Poisson ratios  $\nu_{vh}$ ,  $\nu_{hv}$ , and  $\nu_{hh}$  is given by Eq. (36). As depicted,  $\nu_{vh}$  and  $\nu_{hv}$  increase, while  $\nu_{hh}$  decreases, with  $\sigma_s/P$ , all being divergent at yield. No empirical formulas for the ratios are given in [1], and the two circles in the plot simply depict the values from the inset of Fig. 1. However,  $\nu_{hh} = E_h / (2G_{hh}) - 1$  was assumed to hold by the authors, and, interestingly, it may be derived by taking  $i=h$  and  $j=h$  in Eq. (40), yielding  $\nu_{hh} = E_h / (2\mu) - 1$ .

Assuming that both coefficients  $\mathcal{A}$  and  $\mathcal{B}$  of Eq. (7) are proportional to  $f$  of Eqs. (41)–(44), agreement between experiment and theory is extended to all values of the void ratio. Comparison was also made to Kuwano and Jardine's

data gained using glass ballotini [1]. Taking  $\mathcal{A}=4200$  and  $\mathcal{B}=\frac{5}{3}\mathcal{A}=7000$ , we find similar agreement.

## VI. THE ELASTIC PART OF FLOW RULES

The increment relation Eq. (4) may also be written in the matrix form  $d\vec{\sigma}=\hat{M}d\vec{u}$ , with  $\hat{M}$  a symmetric  $6\times 6$  matrix, and  $d\vec{\sigma},d\vec{u}$  still given as in Eq. (31). The determinant  $\det\hat{M}=9\mathcal{A}^5(2\mathcal{B}\Delta^2-\mathcal{A}u_s^2)\Delta$ , calculated from Eq. (26), vanishes at the yield surface,  $\mathcal{A}u_s^2=2\mathcal{B}\Delta^2$ , because an eigenvalue, call it  $m_1$ , also does. This is not a coincidence, as  $\hat{M}$  is the Jacobian matrix of the energy function, which is positive only in the stable region. [Incidentally, the determinant of the Bousinesq model,  $\det\hat{M}=9\mathcal{A}^5(3\mathcal{B}+4\mathcal{A})\Delta^3$ , never vanishes.] The associated eigenvector  $\vec{m}_1$  points along the direction at which a finite deformation  $d\vec{u}\neq\vec{0}$  may take place under constant stress  $d\sigma_{ij}=0$ . Since  $\vec{m}_1\parallel d\vec{u}$  is only the elastic contribution to the strain, we shall refer to  $\vec{m}_1$  as the elastic flow direction. Setting  $d\sigma_{ij}=0$  in Eq. (4) and using  $\mathcal{A}u_s^2=2\mathcal{B}\Delta^2$ , we obtain

$$du_{ij}=-\frac{1}{2}\left(\delta_{ij}+\frac{u_{ij}}{\Delta}\right)d\Delta=\left(\sqrt{\frac{\mathcal{B}}{2\mathcal{A}}}\frac{\sigma_{ij}^0}{\sigma_s}-\frac{\delta_{ij}}{3}\right)d\Delta.$$

This  $du_{ij}\rightarrow d\vec{u}$  is the eigenvector  $\vec{m}_1$ . Remarkably, one can rewrite this equation as  $du_{ij}/d\Delta=\partial g/\partial\sigma_{ij}$ , or

$$\vec{m}_1\parallel\partial g/\partial\vec{\sigma}\quad\text{with}\quad g=\sqrt{\mathcal{B}/2\mathcal{A}}\sigma_s-P, \quad (45)$$

implying that the elastic flow direction is perpendicular to the yield surface, as defined by the equation  $g=0$ . If the total flow direction is perpendicular to the yield surface, it is referred to as an *associated flow rule* [13,14]. The fact that in granular media flow rules are not typically associated is therefore the result of plastic contributions, which we shall consider, employing the approach of [6], in a future presentation.

## VII. CONCLUSION

For vanishing stress or strain increments, granular media become increasingly reversible and elastic, and can be described by a typical elastic stress-strain relation

$$d\sigma_{ij}=\frac{\partial\sigma_{ij}}{\partial u_{kl}}du_{kl}\equiv\frac{\partial^2w}{\partial u_{kl}\partial u_{ij}}du_{kl}. \quad (46)$$

Using the simple energy expression  $w=(\mathcal{B}\frac{2}{3}\Delta^2+\mathcal{A}u_s^2)\sqrt{\Delta}$ , employed previously to determine static stress distributions in silos and sand piles and under point loads, we find that the calculated response is satisfactorily realistic when compared with the extensive experimental data of Kuwano and Jardine [1].

For increasing stress or strain increments, granular media become successively plastic, i.e., softer, less reversible, and incrementally nonlinear. They then enter a rate-independent region frequently accounted for by the *hypoplastic model* [5]. By allowing the above elastic stress  $\sigma_{ij}=-\partial w/\partial u_{ij}$  to relax,

we were able to reproduce the basic structure of this model, and find quantitative agreement with its predictions—based essentially on the accuracy and appropriateness of the derived quantity  $M_{ijkl}\equiv\partial^2w/\partial u_{kl}\partial u_{ij}$  (see [6]).

## APPENDIX: ENERGETIC STABILITY

In the main text, we considered the convexity of the energy with respect to the variables  $u_s$  and  $\Delta$ . The convexity with respect to  $u_{ij}$  is relevant. As the transformation between these two sets of variables is nonlinear, we bear the burden of proof that both are equivalent.

Thermodynamic stability requires the elastic energy to be a convex function of its six strain variables, or linear combinations of them. This means that all eigenvalues of the Jacobian matrix  $\partial^2w/\partial X_\alpha\partial X_\beta$  are positive. We take  $X_1=u_{xy}$ ,  $X_2=u_{xz}$ ,  $X_3=u_{yz}$ ,  $X_4=(u_{xx}-u_{zz})/2$ ,  $X_5=(u_{xx}-2u_{yy}+u_{zz})/(2\sqrt{3})$ , and  $X_6=-u_{xx}-u_{yy}-u_{zz}$ , with  $Q=u_s^2=2\sum_{\alpha=1}^5X_\alpha^2$ . For an energy of the form  $w=w(\Delta,Q)=w(X_6,Q)$  and denoting  $f\equiv 4\partial w/\partial Q$ ,  $a\equiv\partial^2w/\partial\Delta^2$ ,  $b\equiv 4\partial^2w/\partial Q\partial\Delta$ , and  $c\equiv 16\partial^2w/\partial Q^2$ , the Jacobian matrix is

$$\begin{pmatrix} f+cX_1^2 & cX_1X_2 & cX_1X_3 & cX_1X_4 & cX_1X_5 & bX_1 \\ cX_1X_2 & f+cX_2^2 & cX_2X_3 & cX_2X_4 & cX_2X_5 & bX_2 \\ cX_1X_3 & cX_2X_3 & f+cX_3^2 & cX_3X_4 & cX_3X_5 & bX_3 \\ cX_1X_4 & cX_2X_4 & cX_3X_4 & f+cX_4^2 & cX_4X_5 & bX_4 \\ cX_1X_5 & cX_2X_5 & cX_3X_5 & cX_4X_5 & f+cX_5^2 & bX_5 \\ bX_1 & bX_2 & bX_3 & bX_4 & bX_5 & a \end{pmatrix}$$

with its six eigenvalues given as  $f_{1-4}=f$  and

$$f_{\pm}=\frac{f+a}{2}+\frac{cQ}{4}\pm\frac{1}{2}\sqrt{\left(f-a+\frac{cQ}{2}\right)^2+2b^2Q}. \quad (A1)$$

They are all positive if, and only if,  $f>0$ ,  $2af+acQ-b^2Q>0$ , and  $f+a+cQ/2>0$ , or equivalently

$$\frac{\partial w}{\partial Q}>0, \quad 4\frac{\partial w}{\partial Q}+\frac{\partial^2w}{\partial\Delta^2}+8Q\frac{\partial^2w}{\partial Q^2}>0, \quad (A2)$$

$$\frac{\partial^2w}{\partial\Delta^2}\frac{\partial w}{\partial Q}+2Q\frac{\partial^2w}{\partial Q^2}\frac{\partial^2w}{\partial\Delta^2}-2Q\left(\frac{\partial^2w}{\partial Q\partial\Delta}\right)^2>0. \quad (A3)$$

Because  $u_s^2=Q$ , or  $2u_s(\partial w/\partial Q)=\partial w/\partial u_s$ ,  $2u_s(\partial^2w/\partial\Delta\partial Q)=\partial^2w/\partial\Delta\partial u_s$ ,  $4u_sQ\times(\partial^2w/\partial Q^2)=u_s(\partial^2w/\partial u_s^2)-\partial w/\partial u_s$ , these conditions are equivalent to Eqs. (11) and (12), or

$$\frac{\partial w}{\partial\Delta}>0, \quad \frac{\partial^2w}{\partial\Delta^2}>0, \quad \frac{\partial^2w}{\partial u_s^2}>0, \quad (A4)$$

$$\frac{\partial^2w}{\partial\Delta^2}\frac{\partial^2w}{\partial u_s^2}>\left(\frac{\partial^2w}{\partial u_s\partial\Delta}\right)^2. \quad (A5)$$



For the energy of Eq. (7), the inequalities (A4) imply  $\mathcal{A} > 0$ ,  $\mathcal{B} > 0$ , while Eq. (A5) gives the yield condition (13). Using  $P = \partial w / \partial \Delta$  and  $\sigma_s = \partial w / \partial u_s$ , we can also write Eqs. (A4) and (A5) as

$$\left( \frac{\partial P}{\partial \Delta} \right)_{u_s} > 0, \quad \left( \frac{\partial \sigma_s}{\partial u_s} \right)_{\Delta} > 0, \quad (\text{A6})$$

$$\left( \frac{\partial P}{\partial \Delta} \right)_{u_s} \left( \frac{\partial \sigma_s}{\partial u_s} \right)_{\Delta} > \left( \frac{\partial P}{\partial u_s} \right)_{\Delta}^2. \quad (\text{A7})$$

The Maxwell relation  $\partial P / \partial u_s|_{\Delta} = \partial \sigma_s / \partial \Delta|_{u_s}$  and the identities  $\partial P / \partial \Delta|_{u_s} = \partial P / \partial \Delta|_{\sigma_s} + (\partial P / \partial \sigma_s|_{\Delta}) \partial \sigma_s / \partial \Delta|_{u_s}$ ,  $\partial P / \partial u_s|_{\Delta} = (\partial P / \partial \sigma_s|_{\Delta}) \partial \sigma_s / \partial u_s|_{\Delta}$ , imply an alternative stability condition,

$$(\partial P / \partial \Delta)_{\sigma_s} > 0. \quad (\text{A8})$$

- 
- [1] R. Kuwano and R. J. Jardine, *Geotechnique* **52**, 727 (2002).  
 [2] D. O. Krimer, M. Pfitzner, K. Bräuer, Y. Jing, and M. Liu, *Phys. Rev. E* **74**, 061310 (2006); K. Bräuer, M. Pfitzner, D. O. Krimer, M. Mayer, Y. Jiang, and M. Liu, *ibid.* **74**, 061311 (2006); Y. M. Jiang and M. Liu, *Eur. Phys. J. E* **22**, 255 (2007).  
 [3] F. Alonso-Marroquin and H. J. Herrmann, *Phys. Rev. Lett.* **92**, 054301 (2004).  
 [4] L. D. Landau and E. M. Lifshitz, *Theory of Elasticity*, 3rd ed. (Pergamon Press, New York, 1986).  
 [5] D. Kolymbas, *Introduction to Hypoplasticity* (Balkema, Rotterdam, 2000).  
 [6] Y. M. Jiang and M. Liu, *Phys. Rev. Lett.* **99**, 105501 (2007).  
 [7] G. Gudehus, in *Constitutive Relations for Soils*, edited by G. Gudehus, F. Darve, and I. Vardoulakis (Balkema, Rotterdam, 1984).  
 [8] P. Evesque and P. G. de Gennes, *C. R. Acad. Sci., Ser. IIB Mec. Phys. Astron.* **326**, 761 (1998); P. G. de Gennes, *Rev. Mod. Phys.* **71**, S374 (1999).  
 [9] J. D. Goddard, *Proc. R. Soc. London, Ser. A* **430**, 105 (1990).  
 [10] Y. M. Jiang and M. Liu, *Phys. Rev. Lett.* **91**, 144301 (2003); **93**, 148001 (2004).  
 [11] H. B. Callen, *Thermodynamics* (John Wiley & Sons, New York, 1960).  
 [12] P. G. de Gennes, *Europhys. Lett.* **35**, 145 (1996).  
 [13] A. Schofield and P. Wroth, *Critical State Soil State Mechanics* (McGraw-Hill, London, 1968).  
 [14] W. X. Huang, *Engineering Properties of Soil* (Hydroelectricity Publishing, Beijing, 1983) (in Chinese).  
 [15] A. E. H. Love, *A Treatise on the Mathematical Theory of Elasticity* (Dover, New York, 1927).